Supporting Information

Polechová and Barton 10.1073/pnas.1421515112

SI: Individual-Based Model

We test the predictive power of the derived key parameters using individual-based simulations. Individuals are distributed among demes that form a 1D habitat, with the phenotypic optimum varying along the habitat, and experience a life cycle consisting of selection, mutation, recombination, and then dispersal. Distance is measured in demes, and time in generations. Every generation, each individual mates with a partner drawn from the same deme, with probability proportional to its fitness, to produce a number of offspring drawn from a Poisson distribution with mean of $Exp[r]$, where r is the individual's Malthusian fitness in continuous time. Generations are nonoverlapping. Individual fitness declines due to deviation of the phenotypic trait (z) from the optimum and due to crowding (fitness is density dependent). The trait is determined by a number of additive diallelic loci, which permits genetic variation to evolve. All parameters are described in Table 1. The model is derived as a limit to continuous time and so applies to a wide range of models that reduce to this limit. In this limit, the rate of spatial dispersal depends only on the variance of distance moved, and the effective population density (for both allele frequency and demographic fluctuations) depends only on the variance of offspring number.

Life Cycle. Discrete-time individual-based simulations are set to correspond to the model with continuous time and space. The life cycle is selection → mutation → recombination → migration.

Dispersal. The habitat is formed by a 1D array of demes. With deme spacing $\delta x = 1$, the population size per deme corresponds to the population density. We assume diffusive migration with a Gaussian dispersal kernel. The tails of the dispersal kernel need to be truncated: we choose truncation at 2 SDs of the dispersal kernel throughout, and adjust the dispersal probabilities following ref. 1 (p. 1,209) so that the discretized dispersal kernel sums to 1, and the variance of dispersal is adjusted correctly. For dispersal per generation at $\sigma = \sqrt{1/2}$, dispersal reduces to a nearest-neighbor migration with a probability of migration left and right of $m = 1/4$.

Selection. Every generation, each individual produces a Poisson number of offspring with mean of the individual's fitness $Exp[(r)]$; where $r = r_m(1 - N/K) - (z-\theta)^2/(2V_s)$, as defined earlier.

Mutation. Mutation rate is set to be small so that its contribution to genetic variance is negligible, but large enough to in principle enable expansion of a species' range over the total time of 5,000 generations. Specifically, it is set to one substitution per the whole population and generation. Genetic variance maintained in a population due to dispersal across environments can be substantially larger than genetic variance maintained by mutation–selection balance in uniform environments. In uniform environments, mutational variance $V_m = \sum_i^{n_l} \mu\ \alpha_i^2$ (where α_i are the allelic effects, and n_l is the number of loci) is robustly estimated to be between about $5 \cdot 10^{-5} V_E$ and $5 \cdot 10^{-3} V_E$ (2). Taking a heritability $h^2 \equiv V_G/(V_G + V_E) = 1/3$, we get V_m between $10^{-4} V_G$ and $10^{-2} V_G$. In our model, genetic variance is inflated due to dispersal across environments, and so V_m/V_G must be yet smaller. Taking the higher limit of $V_m = 10^{-2} V_G$, it follows that μ should be smaller than about $4 \cdot 10^{-3}$. It turns out that, in general, the increase of genetic variance due to mutation cannot be fully included in the predictions, as the contribution of mutation–selection balance cannot be robustly separated from the clinal variation (Fig. S10). A considerably higher genetic variance than $V_{G,mut} = 2\mu\ n_l\ V_s$ (up to the limit of $1/4\alpha^2 n_l$) can arise due inflation of the variance by mutation along existing clines. Therefore, we concentrate on a parameter range where the contribution of mutation to genetic variance is low, which is a biologically plausible range. In our model, genetic variance is maintained by gene flow across the environment.

Reproduction, Recombination. The mating partner is drawn from the same deme, with the probability proportional to its fitness. Selfing is allowed at no cost. The genome is haploid with unlinked loci (the probability of recombination between any two loci is 1/2); the allelic effects α_i of the loci combine in an additive fashion.

Simulation Runs. Evolution starts with a well-adapted population at the center of the habitat. The habitat is about 10 cline widths wide; the number of genes is chosen so that, with all genes adapted, the population spans the whole habitat, and that there are enough genes to maintain the "optimal" variance $V_G = b\sigma\sqrt{V_S}$ at the central part of the habitat. At the start of the simulation, one-half of the genes are adapted: their clines take the form and spacing as assumed for the deterministic model under linkage equilibrium.

The population evolves for 5,000 generations; in total, we recorded over a thousand runs where without genetic drift the local population density would be greater than 4 assuming uniform adaptation (such that trait mean matches the optimum). We a priori eliminated very small local population sizes ($N < 4$) so that the population size within a generational dispersal is not excessively small. The parameters were first varied one at a time, and then we tested the threshold drawing the parameters from distributions consistent with our knowledge of the range expected in nature (ref. 3, discussion). The latter will be referred to as the "random" set, with 1,000 runs. The Mathematica code for the simulations, including the distributions used to draw the unscaled parameters for the "random" set, is provided in Dataset S1. Fig. S1 shows the realized distributions for both the unscaled parameters and compound parameters.

SI: Linkage Equilibrium

Stabilizing selection on a quantitative trait generates negative linkage disequilibrium, whereas dispersal generates positive linkage disequilibrium. Felsenstein's (4) analysis of variance components showed that, at equilibrium, the linkage disequilibrium generated by dispersal cancels out with the negative linkage disequilibrium generated by stabilizing selection.

The argument extends to a quantitative trait determined by many diallelic loci, here demonstrated for a haploid genome. The genetic variance is $V_G = \sum \alpha_i^2 p_i(x) q_i(x) + 2\sum_{i \neq j} \alpha_i \alpha_j D_{ij}$. The increase of linkage disequilibrium at quasi-linkage equilibrium (5) between dispersal with variance σ^2 and recombination r_{ij} is given by $D_{ij|disp} = (\sigma^2/r_{ij})(dp_i/dx)(dp_j/dx)$ (6). With allele frequencies at equilibrium, the linkage disequilibrium generated by stabilizing selection alone is $D_{ij|sel} = \left(-r + \sqrt{r_{ij}^2 + 4(1-r_{ij})\alpha_i\alpha_j/V_s\ p_i q_i p_j q_j}\right) \Big/ 2(1-r_{ij}) \sim -\alpha_i\alpha_j/(r_{ij}V_s)\ p_i q_i p_j q_j$ for D_{ij} small.

In this first-order approximation, the terms cancel for each pair of loci when the cline shape is the same as that under linkage equilibrium (ref. 7, two-allele model)—independently of the cline spacing across space: $D_{ij} \equiv D_{ij|disp} + D_{ij|sel} = 0$. This is because $dp_i/dx = p_i q_i\ 4/w_i$, and the cline width at linkage equilibrium is $w_i = 4\sigma\alpha_i/\sqrt{V_s}$.

It may be that the cline width w_i or the linkage disequilibrium is distorted by additional forces, and/or by strong selection—then the linkage disequilibrium components due to dispersal and selection may not cancel. However, unless selection is strong, the first-order approximation gives a simple prediction for the pairwise disequilibrium: $D_{ij} = D_{ij|disp} + D_{ij|sel} = \frac{\sigma^2}{r_{ij}} p_i q_i p_j q_j 16/(w_i w_j) - \alpha_i \alpha_j / (r_{ij} V_s)\ p_i q_i p_j q_j$. For example, we can expect that positive linkage disequilibrium D_{ij}, generated by long-range dispersal, would drive steeper clines.

1. Polechová J, Barton NH (2005) Speciation through competition: A critical review. *Evolution* 59(6):1194–1210.
2. Houle D, Morikawa B, Lynch M (1996) Comparing mutational variabilities. *Genetics* 143(3):1467–1483.
3. Polechová J, Barton N (2011) Genetic drift widens the expected cline but narrows the expected cline width. *Genetics* 189(1):227–235.
4. Felsenstein J (1977) Multivariate normal genetic models with a finite number of loci. *Proceedings of the International Conference on Quantitative Genetics*, eds Pollak E, Kempthorne O, Bailey Jr T (Iowa State Univy Press, Ames, IA), pp 227–245.
5. Barton NH, Turelli M (1991) Natural and sexual selection on many loci. *Genetics* 127(1): 229–255.
6. Barton NH (1986) The maintenance of polygenic variation through a balance between mutation and stabilizing selection. *Genet Res* 47(3):209–216.
7. Barton N (2001) Adaptation at the edge of a species' range. *Integrating Ecology and Evolution in a Spatial Context*, eds Silvertown J, Antonovics J (Blackwell, London), pp 365–392.

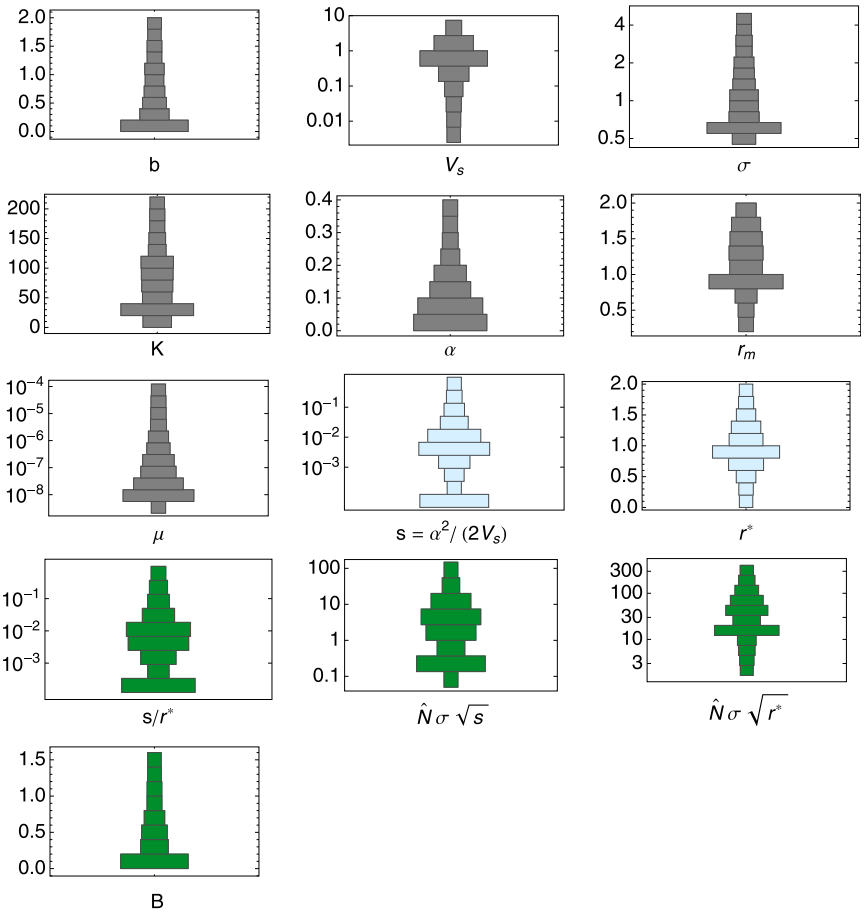

Fig. S1. Distribution of parameters used in the "random set," as described in Table 1. Gray: all unscaled parameters. Light blue: composite parameters. Dark green: scale-free parameters [both s/r^* and $1/(\hat{N}\sigma\sqrt{r^*})$ are given for a reference, although one of them is always redundant; *Materials and Methods*, *Rescaling*].

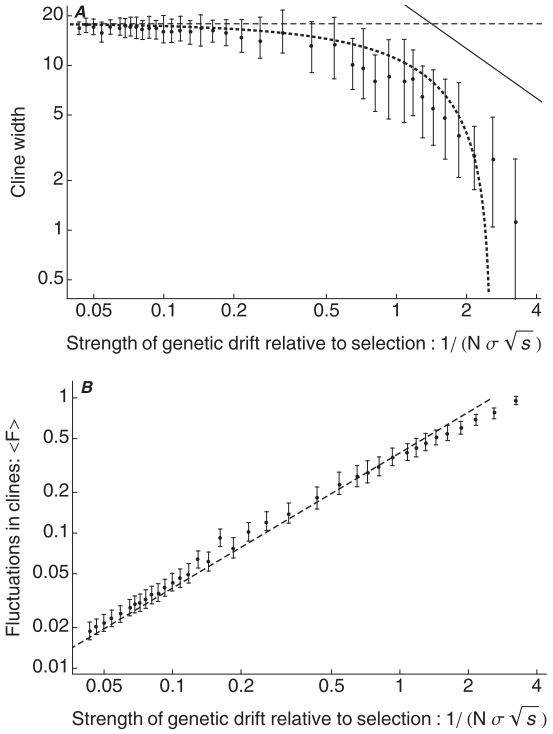

Fig. S2. Cline width decreases as genetic drift gets stronger relative to selection. (*A*) Cline width, defined as a measure of total heterozygosity across space ($w \equiv 4 \int p\, q$), is approximated by $w = w_s(1 - 0.392/(N\sigma\sqrt{s}))$ (thick dotted line; method from ref. 1, supplementary text). Dots give the median cline width across loci with their positive and negative SDs. The dashed horizontal line gives the deterministic cline width, $w_s = 4\sigma/\sqrt{2s}$ (2, 3). As the genetic drift gets very strong relative to selection, the predictions diverges (*Bottom Right*): for very weak selection, the neutral limit $\langle w_0 \rangle \to 4\sigma^2 N$ is approached (solid diagonal line; from ref. 4). Note that genetic variance decreases with the same factor as cline width. (*B*) The decrease in cline width can be understood from the rise in fluctuations of each cline—as fluctuations increase, allele frequencies fix locally and the cline steepens. Fluctuations in clines $\langle F \rangle$ rise approximately with $\langle F \rangle = 0.392/(N\sigma\sqrt{s})$, shown by a dashed line. $\langle F \rangle$ is the variance in allele frequencies scaled by the expected allele frequency, averaged across space, therefore ranging between 0 and 1: $\langle F \rangle \equiv \int_{-\infty}^{\infty} var(p(x,t))dx / \int_{-\infty}^{\infty} \langle p(x,t) \rangle \langle q(x,t) \rangle dx$ (ref. 1, p. 228). Note that these formulae apply only to 1D habitats: as the width of the second (selectively neutral) spatial dimension of the habitat increases, the predictions will start to differ because the effect of genetic drift on a cline depends only weakly on selection in 2D habitats (5). Parameters: $b = 0.1$, $\sigma^2 = 1/2$, $V_s = 2$, $r_m = 1.025$, $\alpha = 1/\sqrt{20}$, $\mu = 10^{-4}$, carrying capacity K increases from 4 to 260.

1. Polechová J, Barton N (2011) Genetic drift widens the expected cline but narrows the expected cline width. *Genetics* 189(1):227–235.
2. Haldane JB (1948) The theory of a cline. *J Genet* 48(3):277–284.
3. Slatkin M (1973) Gene flow and selection in a cline. *Genetics* 75(4):733–756.
4. Hallatschek O, Korolev KS (2009) Fisher waves in the strong noise limit. *Phys Rev Lett* 103(10):108103.
5. Barton NH, Depaulis F, Etheridge AM (2002) Neutral evolution in spatially continuous populations. *Theor Popul Biol* 61(1):31–48.

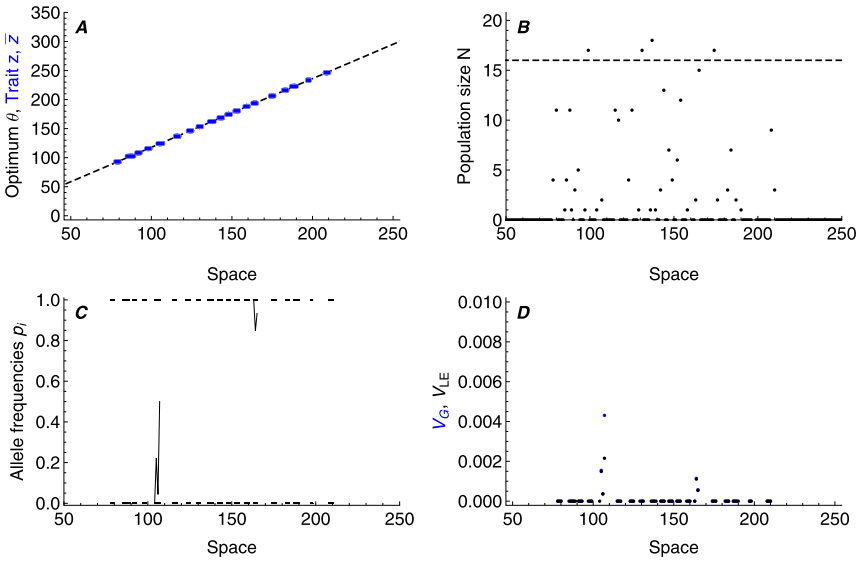

Fig. S3. Species range can fragment when $B > 0.15N\sigma\sqrt{s}$ (Fig. 2), and additionally, $B > \sqrt{2A}$ (Fig. 4). Exact conditions that always lead to range fragmentation were not determined. Fragmented populations are shown in open circles in Figs. 2 and 4. (*A*) Typically, the gradient in trait mean is zero within each fragment. (*B*) Populations are disjunct, and across the habitat, the population size is considerably smaller than predicted for "perfect" adaptation. (*C*) Typically, there is no clinal variation, although transiently, a few clines are maintained. (*D*) Correspondingly, local genetic variance is mostly near zero. Parameters are as follows: $b \doteq 1.18$; $\sigma^2 \doteq 1$, $V_s \doteq 0.44$, $r_m = 1.97$, $K = 29.2$, $\mu = 6 \cdot 10^{-8}$, $\alpha = 0.0093$, time = 5,000 generations (shown at generation 4,800). Note that this fragmentation is not driven by edge effects that arise when population at the carrying capacity reaches the edge of the available habitat, where there is less maladaptive gene flow, which leads to local increase of density, followed by suppression of nearby populations toward the center—and the effect propagates (1). This effect is explained in ref. 2. Here, the simulations are set up such that the population never reaches the margins of the available habitat.

1. Doebeli M, Dieckmann U (2003) Speciation along environmental gradients. *Nature* 421(6920):259–264.
2. Polechová J, Barton NH (2005) Speciation through competition: A critical review. *Evolution* 59(6):1194–1210.

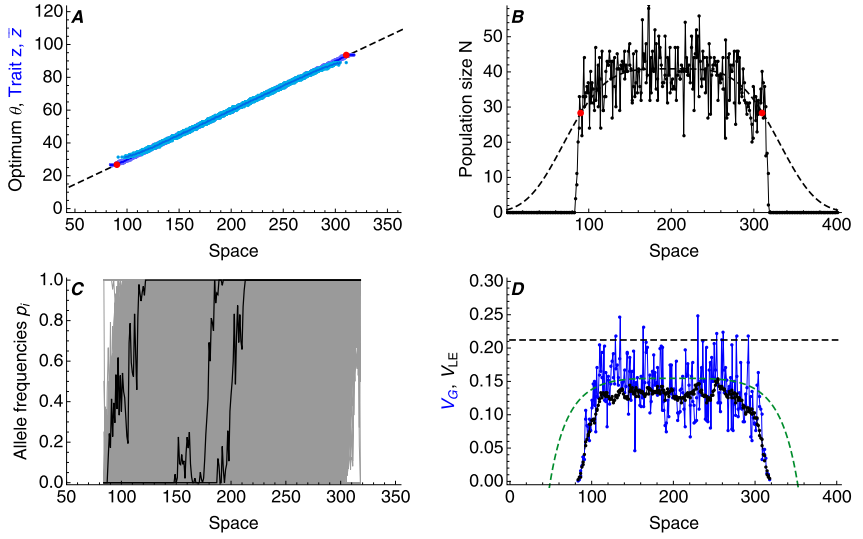

Fig. S4. Nonuniform carrying capacity generates a stable range margin. (*A*) The optimum changes across the environment with a constant gradient $b = 0.3$—the population starts well adapted at the more central part of the habitat (lighter blue). (*B*) The population density declines away from the center—red dots give the predicted failure of the adaptation, based on $B^* = 0.15\ N\sigma\sqrt{s}$. (*C*) Three representative clines are shown in black, and other clines form the gray background (every 10th cline displayed). (*D*) Genetic variance is substantially lower than the deterministic prediction (black dashed line). The dashed green line gives the predicted V^*_{LE} including the effect of genetic drift: $V^*_{LE} = V_{LE}(1 - 0.392/(\hat{N}\sigma\sqrt{s}))$ (Fig. S2). Parameters are as follows: $b = 0.3$, $\sigma^2 = 1/2$, $V_s = 1$, $r_m = 1.1$, $\mu = 10^{-7}$. Population is shown after a stable range margin is reached at time = 100,000 generations (with the exception of the initial distribution of trait values, shown in light blue).

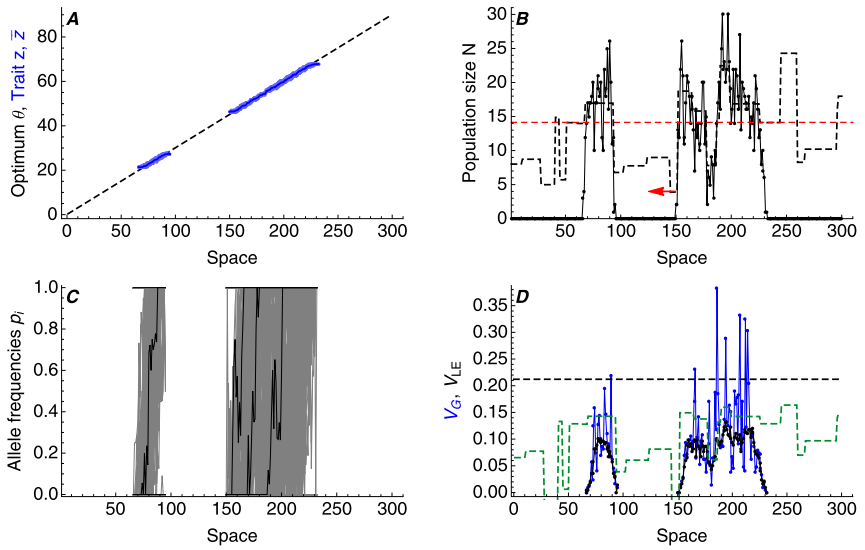

Fig. S5. Species' range is more robust within the already-occupied habitat. A drop in the density to or below the predicted threshold $B^* = 0.15\, N\sigma\sqrt{s}$ (dashed red line in *B*) prevents range expansion. However, a considerably larger drop in the density is necessary before the range fragments within the occupied habitat (*A* and *C*). In this example, species' range contracted from a local drop in the density right in the middle of the range (arrow in *B*), where locally, genetic drift depleted genetic variance to zero. Predicted segregating genetic variance $V_{LE}^* = V_{LE}(1 - 0.392/(\hat{N}\sigma\sqrt{s}))$ is given by green dashed line in *D*. Note that segregating genetic variance $V_{LE} = \sum_i \alpha_i^2 p_i q_i$ (connected black dots, *D*) changes over scales of $\sigma/\sqrt{s}$, whereas population size (*B*) changes over much smaller scales σ. Species' range is more robust to fluctuations within the already-occupied habitat because migration from the neighboring populations stabilizes the species' range; the threshold (dashed red line) predicts when on a linear gradient, species' range would collapse from the margins. Subplot descriptions and deterministic predictions (black dashed lines) are the same as in Fig. 1. Parameters are as follows: $b = 0.3$, $\sigma^2 = 1/2$, $V_s = 1$, $\alpha = \sqrt{1/50}$, $r_m = 1.1$, $\mu = 3 \cdot 10^{-7}$, time = 40,000 generations. At the start of the simulation, population is adapted to the central half of the available habitat. Carrying capacity is generated from a Gaussian distribution centered around the threshold (N^*, dashed red line) with a SD of $N^*/3$; the width of the patches is uniformly distributed between 1 and 30 demes.

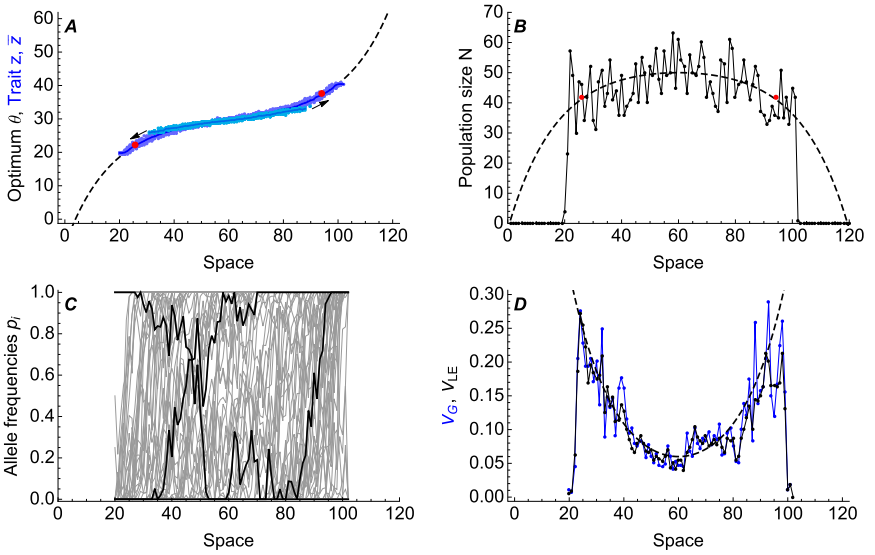

Fig. S6. Sharp margin to a species' range forms even when allelic effects α_i are nonuniform. With exponentially distributed allelic effects α_i, the expansion slows down after 40,000 generations (Fig. S7*A*), at the threshold predicted by mean selection per locus $B^* = 0.15 N\sigma\sqrt{\bar{s}} = 0.34$ (red dots in *A* and *B*). As in this example the allelic effects are not bounded, over very long times, as rare alleles with large effect are recruited (Fig. S7 *B* and *C*), the species' range slowly stretches beyond the threshold B^*. Parameters and subplot descriptions are the same as in Fig. 3—with the exception that the allelic effects are exponentially distributed, with mean $\alpha = \sqrt{1/100}$. (*C*) Note that, when allelic effects vary across loci, occasionally a cline may establish in a reverse direction, correcting a substitution with a large effect on the trait mean. (*D*) As genetic variance V_G increases toward the margins, it evolves to match the ever-steeper environmental gradient: $V_G = b\sigma\sqrt{V_s}$ (prediction shown in dashed line). Gradient in the central habitat is $b = 0.12$; $\sigma^2 = 1/2$, $V_s = 1/2$, $r_m = 1.06$, $K = 50$, $\mu = 2 \cdot 10^{-7}$, time = 100,000 generations (with the exception of the initial distribution of trait values, shown in light blue).

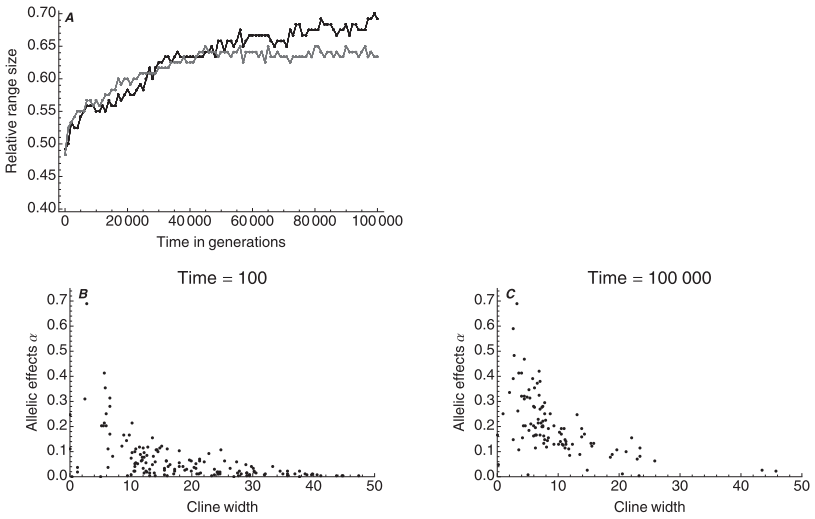

Fig. S7. (*A*) Range expansion slows down near the threshold based on mean selection coefficient even when the allelic effects α_i are nonuniform (black). However, over very long times, further alleles with large effects can be recruited as they are under stronger selection, and species' range expands a little further. (Example from Fig. S6.) The extent of range expansion is only fully bounded by the substitution with the largest selection coefficient that can arise over a given time. For comparison, the rate of range expansion with equal allelic coefficients with $\alpha_i = \overline{\alpha}$ is given in gray (keeping all other parameters same; example from Fig. 3). (*B* and *C*) Over time, genetic drift degrades clines with small allelic effects α. As more alleles with larger effect α contribute to adaptation, clines become narrower and under stronger selection. Parameters are as in Fig. S6. Note that the average selection coefficient is $\overline{s} \equiv \overline{\alpha^2}/2V_s$ and in this example, $s = \alpha$.

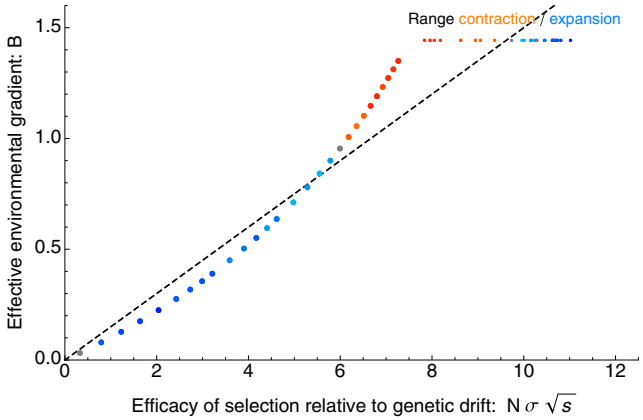

Fig. S8. Adaptation may suddenly fail if dispersal is too large. The threshold for collapse of adaptation (dashed line, $B^* \approx 0.15\, N\sigma\sqrt{s}$) is weakly dependent on dispersal: to the first order, the effect cancels. However, for our model, the strength of density dependence r^* decreases with genetic variance [$r^* = V_G/(2V_s)$], which in turn increases with σ [$r^* \to b\sigma/(2\sqrt{V_s})$]. When r^{*2}/r_m becomes smaller than 1, further increase in dispersal is detrimental as it brings the population closer to the predicted threshold. This is because both $B = b\sigma/(\sqrt{2V_s}r^*)$ and $N\sigma\sqrt{s} = Kr^*/(r_m\,\sigma\sqrt{s})$ are both dependent on r^*—and the effects multiply. The scale for the coloring is adjusted (different to Fig. 2) so that the differences in the rate of range expansion (light to dark blue) and contraction (orange to red) are visible; gray dots again denote population that expanded less than one deme over 5,000 generations. Parameters are as follows: $\sigma = [0.1, 4.24]$, $b = 0.45$, $V_s = 1$, $r^* \equiv 1$ hence $r_m = [1.02, 1.95]$; $K = 28$, $\mu = 4 \cdot 10^{-7}$, $\alpha = \sqrt{1/35}$, time = 5,000 generations.

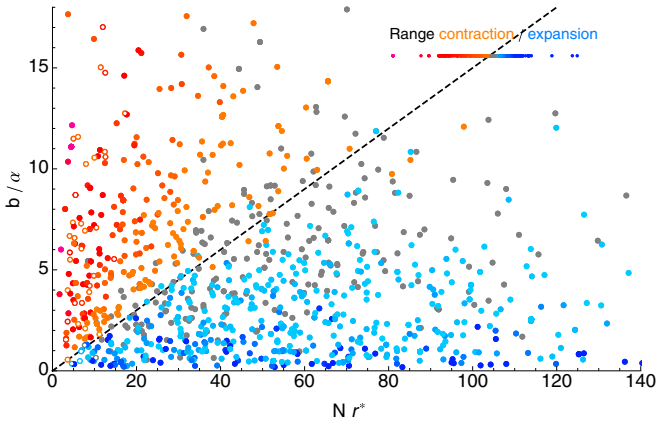

Fig. S9. Alternatively, the threshold for range collapse can be expressed as $b/\alpha \gtrsim 0.15\ Nr^*$. The threshold holds well unless spacing between the clines, α/b, is smaller than about $1/10$—this reflects the limits of our simulation system rather than a biological boundary—the deme-spacing is fixed to $\Delta x \equiv 1$. Data and their depiction are the same as in Fig. 2.

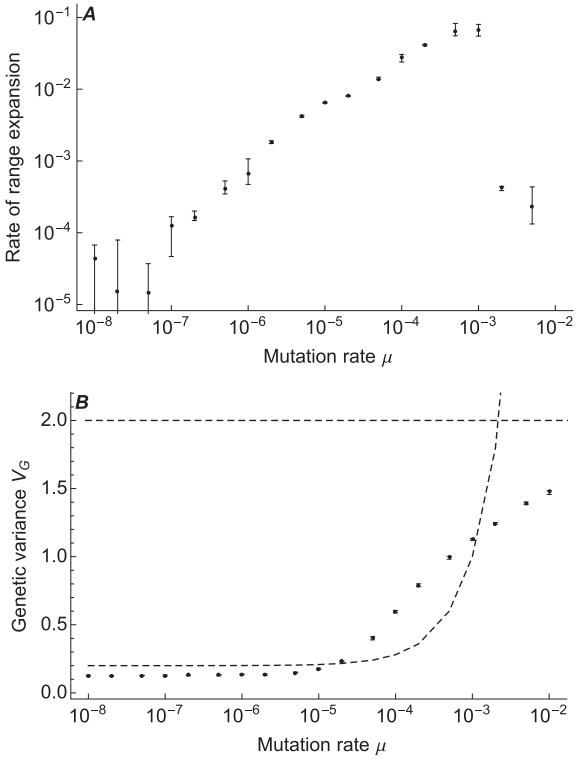

Fig. S10. Effect of mutation rate on the rate of range expansion and local genetic variance. (*A*) Rate of range expansion increases about linearly with mutation rate μ per locus and generation ($5 \cdot 10^{-8} < \mu < 10^{-3}$). When mutation becomes too high, then the rate of expansion first decelerates, and for yet higher mutation rates ($\mu \gtrsim 10^{-2}$), the population starts to collapse (cf. ref. 1). Note that, in general, mutation rate per locus and generation is expected to be lower than about 10^{-4} (*SI: Individual-Based Model*). (*B*) Local genetic variance V_G increases with mutation rate. For low-to-moderate mutation rates, genetic variance is maintained by mixing across the phenotypic gradient, $V_G = b\sigma\sqrt{V_s}$. The dashed curve gives the prediction $b\sigma\sqrt{V_s} + 2\mu\ n_l V_s$, which assumes the components of genetic variance due to gene flow (first term) and mutation–selection balance (second term) combine additively, whereas all n_l loci are at linkage equilibrium: the mismatch between the dashed curve and the realized genetic variance implies that, with clinal variation, $\mu \ll s$ is not a sufficient condition for the contribution of mutation to be negligible. The top dashed line gives the maximum variance possible, $1/4\ n_l\ \alpha^2$ (where α is a phenotypic effect of a single substitution). With increasing variance, population density drops steadily (not shown): eventually, species' range starts to contract and population collapses. Parameters are as follows: $b = 0.4$, $\sigma^2 = 1/2$, $V_s = 1/2$, $r_m = 1.06$, $K = 50$, $\alpha = s = 0.01$, 800 genes. Initial population spans over 100 demes, and population evolves over 5,000 generations. For both plots, error bars give the SDs.

1. Henry RC, Bartoń KA, Travis JM (2015) Mutation accumulation and the formation of range limits. *Biol Lett* 11(1):20140871.

Other Supporting Information Files

Dataset S1 (NB)